The American Journal of Pathology, Vol. 184, No. 10, October 2014

The American Journal of
PATHOLOGY
ajp.amjpathol.org

BIOMARKERS, GENOMICS, PROTEOMICS, AND GENE REGULATION

Single-Cell Genetic Analysis Reveals Insights into Clonal Development of Prostate Cancers and Indicates Loss of *PTEN* as a Marker of Poor Prognosis

Kerstin M. Heselmeyer-Haddad,* Lissa Y. Berroa Garcia,* Amanda Bradley,* Leanora Hernandez,* Yue Hu,* Jens K. Habermann,† Christoph Dumke,† Christoph Thorns,‡ Sven Perner,§ Ekaterina Pestova,¶ Catherine Burke,‖ Salim A. Chowdhury,**†† Russell Schwartz,†††‡‡ Alejandro A. Schäffer,§§ Pamela L. Paris,‖ and Thomas Ried*

From the Genetics Branch, Center for Cancer Research, National Cancer Institute, and the Computational Biology Branch,§§ National Center for Biotechnology Information, the National Institutes of Health, Bethesda, Maryland; the Section for Translational Surgical Oncology and Biobanking,† Department of Surgery, and the Institute of Pathology,‡ University of Lübeck and University Medical Center Schleswig-Holstein, Campus University of Lübeck, Lübeck, Germany; the Department of Prostate Cancer Research,§ Institute of Pathology, University Hospital of Bonn, Bonn, Germany; Abbott Molecular,¶ Des Plaines, Illinois; the Department of Urology,‖ Helen Diller Family Comprehensive Cancer Center, University of California at San Francisco, San Francisco, California; and the Joint Carnegie Mellon/University of Pittsburgh Ph.D. Program in Computational Biology,** the Lane Center for Computational Biology,†† and the Department of Biological Sciences,‡‡ Carnegie Mellon University, Pittsburgh, Pennsylvania

Accepted for publication June 16, 2014.

Address correspondence to Kerstin M. Heselmeyer-Haddad, Ph.D., Genetics Branch, Center for Cancer Research, National Cancer Institute, NIH, 50 South Dr, Bldg 50, Room 1408, Bethesda, MD 20892. E-mail: heselmek@mail.nih.gov.

Gauging the risk of developing progressive disease is a major challenge in prostate cancer patient management. We used genetic markers to understand genomic alteration dynamics during disease progression. By using a novel, advanced, multicolor fluorescence *in situ* hybridization approach, we enumerated copy numbers of six genes previously identified by array comparative genomic hybridization to be involved in aggressive prostate cancer [*TBL1XR1*, *CTTNBP2*, *MYC* (alias c-*myc*), *PTEN*, *MEN1*, and *PDGFB*] in six nonrecurrent and seven recurrent radical prostatectomy cases. An *ERG* break-apart probe to detect *TMPRSS2-ERG* fusions was included. Subsequent hybridization of probe panels and cell relocation resulted in signal counts for all probes in each individual cell analyzed. Differences in the degree of chromosomal and genomic instability (ie, tumor heterogeneity) or the percentage of cells with *TMPRSS2-ERG* fusion between samples with or without progression were not observed. Tumors from patients that progressed had more chromosomal gains and losses, and showed a higher degree of selection for a predominant clonal pattern. *PTEN* loss was the most frequent aberration in progressers (57%), followed by *TBL1XR1* gain (29%). *MYC* gain was observed in one progresser, which was the only lesion with an *ERG* gain, but no *TMPRSS2-ERG* fusion. According to our results, a probe set consisting of *PTEN*, *MYC*, and *TBL1XR1* would detect progressers with 86% sensitivity and 100% specificity. This will be evaluated further in larger studies. *(Am J Pathol 2014, 184: 2671–2686; http://dx.doi.org/10.1016/j.ajpath.2014.06.030)*

Prostate cancer is the most commonly diagnosed noncutaneous neoplasm among US males (238,590 estimated cases in 2013) and is the second leading cause of cancer-related deaths (29,720 estimated deaths).[1] Disease incidence exceeds mortality by a factor of 8; this suggests that many prostate cancers do not result in disease-associated death. This observation is attributable to the fact that many prostate cancers do not progress to metastatic disease. Patients with more indolent tumors would benefit from an active surveillance approach. Men with aggressive disease, however,

Supported in part by the Intramural Research Program of the NIH, National Cancer Institute, US National Library of Medicine, and NIH R01 Awards CA140214, AI076318, and CA115484.

Disclosures: FISH probes were provided by Abbott Molecular under the terms of a Material Transfer Agreement. E.P. is an employee of Abbott Molecular. T.R. and K.M.H.-H. hold a patent for the detection of cervical carcinomas (US 5919624), which has been licensed to Abbott Molecular and other companies.

Portions of this work have been accepted for presentation at the 64th Annual Meeting of the American Society of Human Genetics in San Diego, CA, October 18-22, 2014.

http://dx.doi.org/10.1016/j.ajpath.2014.06.030

need immediate and often adjuvant therapy after radical prostatectomy (RP) to improve survival. Although serum-level screening for prostate-specific antigen (PSA) has increased detection of prostate cancer at earlier stages,[2] sensitive and specific tests to distinguish men with indolent disease from men with aggressive prostate cancers are still lacking, which generates a dilemma in how to adapt risk-associated treatments.[3]

Numerous studies have identified genomic changes as potential predictors of progression.[3–8] Perhaps the best-known tumor marker specific to prostate cancer is the fusion of *TMPRSS2* and *ERG* on chromosome 21.[9] Fusions of these two genes have been observed in approximately 30% to 60% of prostate cancers,[9–17] but whether the gene fusion predicts tumor progression is controversial.[12,18,19] One explanation might be that many possible *TMPRSS2-ERG* fusions exist, which result in transcripts with different consequences for disease prognostication.[13,20–22] An additional problem in elucidating the role of *TMPRSS2-ERG* in tumor progression might be intratumor heterogeneity.[23–25]

Deep sequencing of somatic mutations[26–28] and approaches to enumerate copy number variation on the level of single cells[29–31] in cancer have led to increasing recognition of the importance of such intratumor heterogeneity in cancer progression. Herein, we explore intratumor heterogeneity of prostate tumors using a special break-apart probe for the *TMPRSS2-ERG* fusion[10] and six single-gene probes selected on the basis of a prior array comparative genome hybridization (aCGH) study.[32] Paris et al[32] screened prostate cancers treated with RP from patients with similar high recurrence risk, but different clinical outcomes, for chromosomal aberrations with aCGH. Comparison with an independent set of metastases revealed approximately 40 candidate markers associated with metastatic potential. For the current study, we chose six of these markers (listed herein in chromosome order)—*TBL1XR1* (3q26.23), *CTTNBP2* (7q31.2), *MYC* (alias c-*myc*; 8q24.21), *PTEN* (10q23.1), *MEN1* (11q13), and *PDGFB* (22q13.1)—to be tested for their potential use as indicators of progressive disease. The markers and two centromeric control/enumerator probes (CEP8 and CEP10) were applied as fluorescence *in situ* hybridization (FISH) probes to single-cell suspensions prepared from archived formalin-fixed, paraffin-embedded (FFPE) material for a subset of cases from the original study[32] (ie, seven prostate cancers from patients with recurrence and six tumors from patients without recurrence after RP). Our novel approach of multiplexing FISH probes[31] allowed signal enumeration in the same cells.

Probes were selected on the basis of the aCGH loci mapping to a gene. Two of the gene probes represent genes with well-known roles in prostate cancers, *MYC*[33,34] and *PTEN*.[35,36] Many prostate cancer studies have reported the co-occurrence of *TMPRSS2-ERG* fusion and loss of *PTEN*[37,38]; others have reported the co-occurrence of gain of *MYC* and loss of *PTEN*.[39,40] A third gene in our probe set, *MEN1*, is a known cancer-associated gene, but with few studies in prostate cancer. *TBL1XR1*, *CTTNBP2,* and *PDGFB* have rarely been the objects of targeted studies in prostate cancer, but there is evidence supporting their potential relevance to prostate cancer.

Biallelic inactivation of *MEN1* results in multiple endocrine neoplasia, type 1,[41] leading to hormone-related tumors, and *MEN1* is considered to function as a classic tumor suppressor. $Men1^{+/-}$ mice are susceptible to prostate cancer.[42] In human prostate cancer, however, *MEN1* has copy number gains and is usually overexpressed, making it an oncogene.[43,44]

TBL1XR1 is an E3 ubiquitin ligase, which is expressed in the prostate.[45] One of its principal functions is to recruit β-catenin to the promoters of Wnt target genes.[46] The β-catenin binding leads to increased transcription of lymphoid enhancer-binding factor 1 target genes by displacing proteins of the transcriptional repressor family called transducing-like enhancers from lymphoid enhancer-binding factor 1.[47] Evidence implicating increased nuclear location of β-catenin in prostate cancer and its progression includes the following: i) various associations between increased Wnt signaling and prostate cancer metastasis to the bone, ii) somatic mutations in specific regions of *CTNNB1*, the gene encoding β-catenin, in 5% of prostate cancers, iii) significantly increased frequency of positive nuclear staining for β-catenin in prostate cancers, and iv) both direct and indirect regulatory effects of β-catenin binding to the *AR* gene, which encodes the androgen receptor.[48]

As for *MEN1*, whether *TBL1XR1* functions as an oncogene or as a tumor suppressor varies by tumor type. *TBL1XR1* is overexpressed and in a region of recurrent copy number gains in lung cancer[49] and in breast cancer.[50] However, *TBL1XR1* is recurrently mutated or deleted in hematological malignancies,[50] and its expression inhibits the growth of head and neck cancer cells.[45]

Platelet-derived growth factor (*PDGF*) comprises a set of four ligands (PDGFs A, B, C, and D) that bind to two receptors (*PDGFRA* and *PDGFRB*) to deliver signals that affect cell growth, cell shape, and chemotaxis.[51] PDGFRA and PDGFRB, which encode the receptor units, are overexpressed in bone marrow metastases of prostate cancer,[52] and higher PDGFRB expression is part of a five-gene expression-based predictor for prostate cancer recurrence.[53] There is a competition between two of its ligands, PDGFB and PDGFD, in prostate cancer, such that when *PTEN* is lost, PDGFD is preferred.[54]

CTTNBP2 influences the size and number of dendritic spines.[55] *CTTNBP2* has roles in other tissues, including binding of the RAD21-cohesin complex.[56] More specific to prostate cancer, *CTTNBP2* is in a block of genes on chromosome 7 that is differentially methylated in prostate cancer cell lines.[57]

We applied two layers of analysis to this panel of FISH probes. First, we pursued the conventional strategy of profiling the probe set in subsets of tumor samples from RP patients with different clinical outcomes (herein, non-

progressers and progressers) to identify combinations of probes that distinguish patient groups. We also pursued a novel, unconventional goal of building a mathematical model of cellular-level progression for each tumor sample and derived test statistics that can collectively distinguish the two groups of patients.[58] The first goal is fulfilled with a candidate three-probe test, which effectively distinguishes progressers from non-progressers in our study; however, it will require validation in a larger sample. Independent of that, our modeling work provided insights into genome dynamics of prostate cancer progression.

Materials and Methods

Materials

FFPE surgery specimens of prostate carcinomas from six patients with non-progressive disease and seven patients with progressive disease after RP were retrieved from the archives of the Tissue Core at the Helen Diller Family Comprehensive Cancer Center, University of California (San Francisco, CA), using samples designated for research purposes. Recurrence or progressive disease was defined as two consecutive PSA measurements within 1 year of $\geq$0.2 ng/mL and/or evidence of metastatic disease. The clinical data are summarized in Table 1.

The material was prepared using a dividing procedure that has been described previously.[31] The hematoxylin and eosin (H&E)–stained sections were used to verify that each section consisted of at least 50% tumor material. The 50-μm unstained sections were then disintegrated, and cytospins were prepared as described.[31]

In addition, we used three FFPE surgery specimens of prostate carcinomas from the University Medical Center Schleswig-Holstein, Campus Lübeck (Lübeck, Germany), to test a three-color FISH probe panel on tissue sections (4 μm thick) to assess the feasibility of implementing this test in routine pathological analysis.

The material for the current study has been coded, and an exemption has been issued by the NIH Office of Human Subjects Research for use of the de-identified data.

FISH Data

The cytospins were evaluated by FISH with CEPs for centromeres 8 and 10 and six locus-specific identifier probes for the following genes: *TBL1XR1* (3q26.23), *CTTNBP2* (7q31.2), *MYC* (8q24.21), *PTEN* (10q23.1), *MEN1* (11q13), and *PDGFB* (22q13.1) (Abbott Molecular, Des Plaines, IL). The probes were selected on the basis of previous aCGH data,[32] and each probe represented approximately 200 to 600 kb of genomic sequence centered on the gene of interest; the probes were directly labeled with fluorophores. The centromere probes, *PTEN* and *MYC*, were labeled in SpectrumAqua or SpectrumGreen (Abbott Molecular). *CTTNBP2* and *MEN1* were labeled in SpectrumRed, whereas *PDGFB* and *TBL1XR1* were labeled in SpectrumGold. The FISH probes were combined into two panels. The panel for the first hybridization consisted of *CEP10*, *PTEN*, *CTTNBP2*, and *PDGFB*. The panel for the second, subsequent hybridization contained *CEP8*, *MYC*, *MEN1*, and *TBL1XR1*. The samples were also evaluated for their *TMPRSS2-ERG* fusion status with an *ERG* break-apart probe[10] in a third, subsequent hybridization. The *ERG* probe hybridization was recorded in three-digit patterns for each cell, with the first digit registering the number of normal *ERG* alleles (red and green signals on top of each other), the second digit referring to the number of telomeric *ERG* probe signals (single green signals), and the third digit representing the number of centromeric *ERG* probe signals (single red signals). Therefore, a 200 pattern would be indicative of a normal diploid status of *ERG*, whereas a 111

Table 1 Clinical Patient Data

Patient group	Patient no.	Age (years)	PreOp PSA (ng/mL)	Gleason primary	Gleason secondary	Gleason sum	Surgical year	Follow-up duration or time to recur (months)	Margin status	Seminal vesicle involvement	Lymph node involvement	Extracapsular extension
Non-progressers	1	60.4	7.2	3	5	8	1994	72.16	Neg	No	Neg	No
	2	65.8	19.4	3	4	7	1996	30.81	Neg	No	Neg	No
	3	64.4	7.3	3	4	7	2000	78.18	Neg	No	Neg	Yes
	4	52.5	5.1	3	5	8	1998	65.59	Neg	No	Neg	No
	5	63.8	6	3	4	7	1995	63.16	Neg	No	Neg	No
	6	53.8	4.5	4	3	7	2001	55.82	Neg	No	Neg	No
Progressers	7	61.2	11.1	3	4	7	1996	5.03	Pos	No	Neg	Yes
	8	60.4	10.2	3	4	7	2000	2.56	Neg	No	Neg	No
	9	65.8	15.7	3	4	7	2000	3.72	Neg	No	Neg	Yes
	10	64.4	10.9	4	3	7	2002	1.38	Pos	Yes	Neg	Yes
	11	68.6	14.3	4	3	7	2003	9.11	Neg	No	Neg	No
	12	75.2	5.5	3	4	7	2003	45.7	Neg	No	Pos	No
	13	60	24	4	3	7	2003	1.84	Neg	Yes	Pos	Yes

Neg, negative; Pos, positive; PreOp, preoperative.

or a 101 pattern would be indicative of a fusion of *TMPRSS2-ERG* by insertion/translocation or deletion, respectively.[10]

One cytospin per case was hybridized and evaluated with the above mentioned three different probe sets using single-cell FISH methods, as described previously.[31] Detection of the *ERG* break-apart probe was performed according to Perner et al.[10] In all 13 samples, all probes could be counted. This resulted in an eight-probe signal pattern plus a three-digit *TMPRSS2-ERG* pattern for each cell analyzed, with an average of 316 (range, 197 to 372) interphase nuclei counted for each case. As previously described,[31] for each cell, a ploidy value (diploid, triploid, or tetraploid) was assigned to each signal pattern on the basis of the assessment of the pattern. A computer program developed to assign gain and loss patterns by comparing signal counts to the ploidy value[59] was applied, and the patterns were sorted according to their frequency and displayed in color charts giving an overview of the clonal populations and the overall heterogeneity observed in the tumors (Figure 1).[31]

The tissue sections (4 μm thick) were deparaffinized in xylene, hydrated, and pretreated with 0.02% pepsin for 25 to 70 minutes. Slides were then washed in 1× phosphate-buffered saline, dehydrated, air dried, and codenatured at 72°C for 5 minutes with a three-color probe panel consisting of *MYC-TBL1XR1-PTEN*. The probe panel was either labeled in-house by nick translation using Dyomics 415-dUTP (Dyomics, Jena, Germany) for *MYC* or Dyomics 505-dUTP for *TBL1XR1* and SpectrumOrange-dUTP (Abbott Molecular) for *PTEN*, or provided by Abbott Molecular in the following color scheme: *MYC* in SpectrumAqua, *PTEN* in SpectrumGreen, and *TBL1XR1* in SpectrumGold. The slides were detected with a 2-minute wash in 2× standard saline citrate (SSC)/0.3% NP40 at 48°C, followed by 1 minute in 2× SSC/0.1% NP40 and 1 minute in 2× SSC, both at room temperature. Slides were air dried and coverslipped, and images were taken with a Leica DMRXA microscope (Leica, Wetzlar, Germany) equipped with custom filters (Chroma, Bellows Falls, VT) and a CoolSnap camera (Photometrics, Tucson, AZ).

DNA Ploidy Measurements

Nuclear DNA ploidy status was assessed by image cytometry using Feulgen-stained cytospins of dissociated cells from all samples, except for case 10, because of insufficient cell material. The staining procedure, internal standardization, and cell selection criteria were based on published methods.[60] At least 7803 particles per sample (mean, 24,000; range, 7803 to 72,101) were detected automatically using the ICM imaging system (Ahrens ICM Cytometry System; Meβtechnische Beratung, Bargteheide/Hamburg, Germany). At least 603 cells (mean, 2953; range, 603 to 8422) per sample were interactively selected in the ICM cell gallery and quantitatively measured for their DNA content. All DNA values were expressed in relation to the corresponding staining controls (lymphocytes), which were given the value 2c, denoting normal diploid DNA content. The DNA profiles were classified as previously described.[60] Samples were assessed as euploid when <5% of cells showed DNA values >4.5c. Aneuploidy was defined as >5% of cells presenting with DNA values exceeding the tetraploid region (>4.5c).

aCGH Data

The previously acquired aCGH data for regions containing the genes used in our FISH analysis were extracted from the existing data set.[61] The aCGH-based copy number calls for all 13 cases and 6 genes were recorded and aligned with the corresponding FISH calls for the purpose of comparing by correlation analysis of the copy number estimates obtained by aCGH and by FISH.

Analysis of Tumor Heterogeneity

We refer to the ordered list of count values for each probe as a signal count pattern. To explore the possibility that tumors with progression are more or less heterogeneous than tumors without progression, we compared three measures of diversity in the distribution of FISH signal count patterns: i) instability index, ii) Shannon index, and iii) Simpson index.[62] The indices were computed for each sample and were then compared between the progresser and non-progresser distributions by either comparing the mean or using a Wilcoxon signed-rank test. The instability index is defined as 100 times the number of cell count patterns divided by the number of cells. To define the other two indices, let p_i be the probability of the i^{th} cell count pattern. Then, the Shannon index, which is commonly used in information theory (alias entropy), is as follows:

$$-\sum p_i log_2(p_i). \quad (1)$$

The Simpson index, which is commonly used in population genetics, is Σp_i^2.

Estimation of Empirical Significance of a Set of Gene Gains/Losses to Distinguish Non-Progressers versus Progressers

To assign an empirical *P* value for sets of gains and losses that may distinguish non-progressers versus progressers, we used simulation. Permutation tests were performed in which a status of gain/loss/neither for each of the six genes (*TBL1XR1*, *CTTNBP2*, *MYC*, *PTEN*, *MEN1*, and *PDGFB*) was assigned at random to 13 samples, with the progresser/non-progresser status permuted. In each replicate, the number of samples with a gain or loss of each gene was fixed to match the observed data. In this context, a classifier is a nonempty set of gene gains and losses from the six genes that predicts whether a sample comes from a progresser, if at least one of the gains and losses is present, or from a non-

progresser, if at least one of the specified gains and losses is not present. Each gene may be specified as gained, specified as lost, or not used in the classifier. Therefore, there are 729 possible classifiers ($3^6 - 1$). For each replicate r, we considered all possible classifiers. The test statistic A (classifier, r) assigned to a classifier was the arithmetic mean of sensitivity and specificity. For each of the 10,000 replicates r, the test statistic $S(r)$ was the maximum test statistic A among all possible classifiers for fixed r. The empirical P value assigned to a classifier of the observed data was the fraction of replicates r for which the $S(r)$ is greater than or equal to A (classifier, observed data).

Modeling Tumor Progression and Analysis of Node Depth

For each of the 13 tumors, we modeled the progression of copy number changes using FISHtrees software,[58] which infers phylogenetic trees describing progression among the observed cell types as distinguished by their probe copy numbers. A tree is inferred from the data for each tumor to heuristically seek to minimize the total number of copy number changes across the tree. In this analysis, we used the six gene probes and we used the break-apart probe to assess the copy number of *ERG*. We did not use the fusion status or the centromere probes. For each tumor, FISHtrees generated a tree model in which the normal state (2, 2, 2, 2, 2, 2, 2) is at the root of the inferred tree and each edge moving away from the root to a new node corresponds to a change in copy number of one gene. For each node, we also stored the number of cells observed to match the seven-component signal count pattern for that node.

The number of steps away from the root is usually called the depth of a node. Our prior work on cervical cancer progression trees[58] showed that the distribution of cells by depths provides a measure of tree topology that is predictive of progression potential. To test whether this characterization of tree topology is similarly predictive of prostate cancer progression, we performed an analogous test. We computed the percentages of cells represented by nodes at each depth in the tree, as described previously.[58] We used percentages of cells at each depth rather than total cells to normalize for differing numbers of cells analyzed for different tumors. We visualized the distribution of the depths of cells in progressers versus non-progressers by a bar graph. We then tested for significance of the difference between average depths for non-progressers versus progressers by a Wilcoxon signed-rank test. Because we hypothesized that the trees derived from progresser samples would have greater average depth, the Wilcoxon P values were one sided.

Results

In a previously published aCGH study,[32] we identified loci that were differentially gained or lost in primary prostate cancers from patients with non-progressive or progressive disease after RP. A subset of the genes was validated by TaqMan analysis.[32] On the basis of these results and the feasibility of probe design, FISH probes centered on the genes of interest were selected. We hybridized the selected FISH probes targeting the six most promising markers [ie, *TBL1XR1* (3q26.23), *CTTNBP2* (7q31.2), *MYC* (8q24.21), *PTEN* (10q23.1), *MEN1* (11q13), and *PDGFB* (22q13.1)], together with centromere probes for chromosomes 8 and 10 and an *ERG* break-apart probe[10] for determining whether the fusion status of *TMPRSS2-ERG* could serve as an additional progression marker. The probes were sequentially hybridized to interphase cells prepared as cytospins from 13 primary prostate carcinomas (six non-progressers and seven progressers).[63] Signal patterns were counted in 197 to 372 nuclei per sample (average, 316 nuclei), excluding nuclei with two signals for all probes and a 200 pattern (indicating two normal alleles) for the *ERG* break-apart probe.

Clinical Features

Pertinent clinical parameters are summarized in Table 1. All patients were at high risk of recurrence by the D'Amico Risk Classification.[63] No clinical variables were found to be confounding.[61]

Chromosomal Instability and Clonal Patterns

The FISH probe panels were hybridized sequentially to individual nuclei of the same specimen. Repeated hybridization and relocation of the cells afforded us the possibility of enumerating clonal aberration patterns on a cell-to-cell basis for all six gene probes, the two centromere probes, and the *ERG* break-apart probe. The FISH signal patterns were assigned to two groups: patterns for which each cell fitting the pattern had an identical count for all signals, termed signal pattern clones, and patterns for which each cell fitting the pattern matched each other cell in the direction of change (gain, loss, or normal) of each signal but not necessarily in the exact counts, termed imbalance clones. For example, in case 10, the major imbalance clone is gain of *TBL1XR1*, gain of *CTTNBP2*, normal for *MYC*, loss of *PTEN*, normal for *MEN1*, normal for *PDGFB*, and break-apart probe pattern 101 (case 10) (Figure 1). To visualize and compare major imbalance clones in prostate carcinomas with or without progressive disease, each cell of the lesion was displayed according to its *ERG* break-apart patterns and its gain, loss, or unchanged (normal) status, with the gene probes sorted according to their chromosomal location from the top to the bottom of the chart and with the patterns observed displayed from left to right sorted by frequency (Figure 1). In addition, the frequency of gained and lost status for each of the gene loci and each *ERG* break-apart pattern was calculated in percentages of the total cell population, the average ploidy of the lesion, and the average

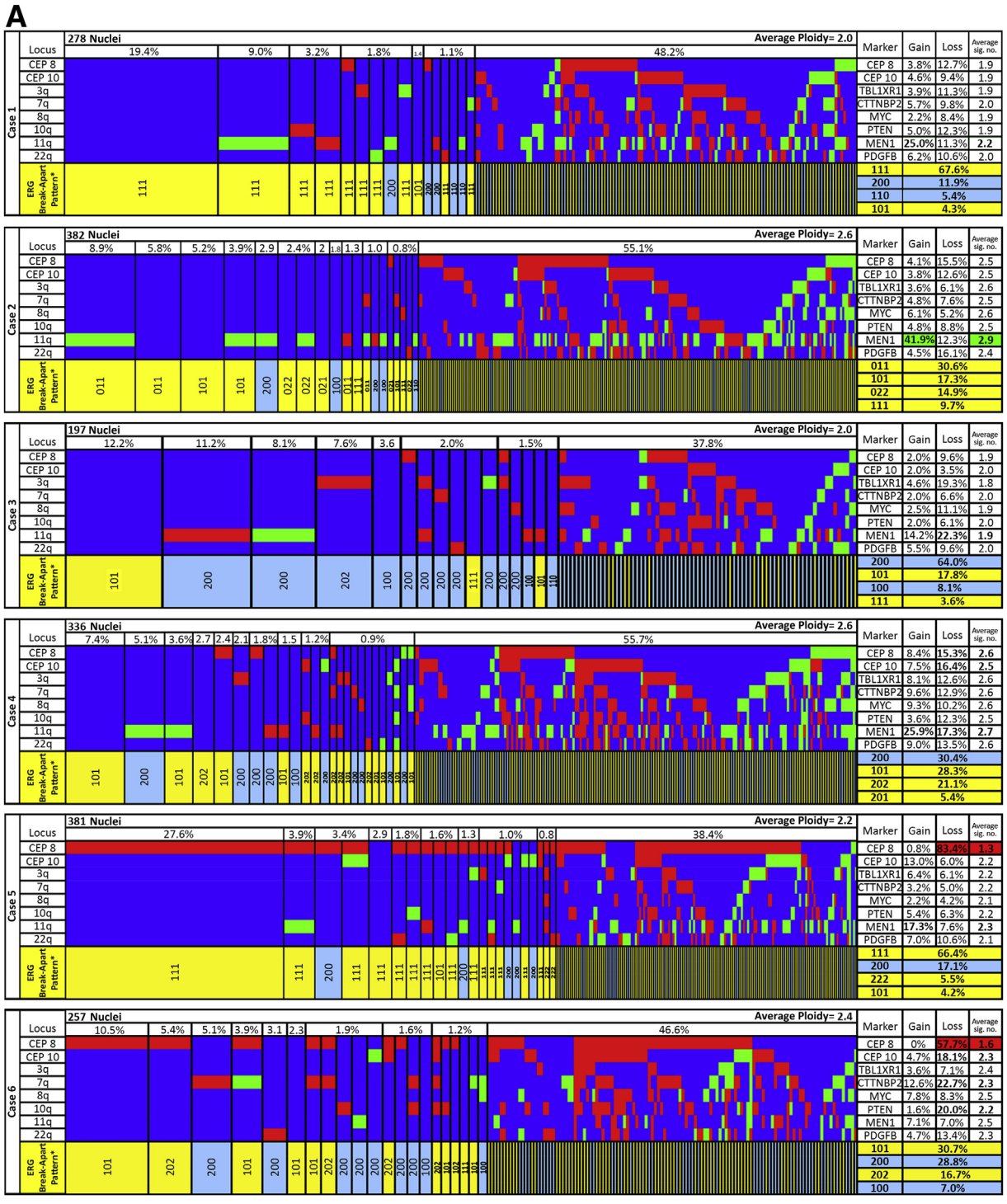

Figure 1 Summary of imbalance clones in six cases of primary prostate carcinoma without progression (cases 1 to 6; **A**) and seven cases with progression (cases 7 to 13; **B**). Green, gains; red, losses; blue, unchanged. The organization of the graphs is the same for all cases and is explained for case 1 in detail from left to right. The Locus column shows the chromosome arm. Each vertical line separates the most common imbalance clones. The row above the imbalance clones displays the percentages at which the clones were found. For example, the most frequent clone in case 1 comprised 19.4% of the cells with an *ERG* break-apart fusion pattern of 111, indicating fusion by insertion, but exhibited no other gains or losses. The second most frequent clone comprised 9.0% of the cells and had the same *ERG* pattern 111 but showed, in addition to that change, a gain of *MEN1*. Two clones that each comprised 3.2% of the tumor cell population followed. Both showed also the 111 pattern for fusion, but one of them had a loss for *PTEN* and the other displayed a loss for *MEN1*. The Marker column shows the gene/probe name. The Gain column shows that 25% of the cells had a gain of *MEN1*. None of the gains and losses comprised >30% of the cell population in case 1. The Average sig. no. column shows that the average signal count for *MEN1* in the entire population was 2.2. The percentage of gains or losses in >30% of the cells is in red (loss) and green (gain), respectively, highlighting (eg, *MEN1* gain in case 2). Two hundred seventy-eight nuclei were counted for case 1. Average ploidy values were calculated from the ploidy values assigned to each nucleus by signal patterns (as described in *Materials and Methods*). The numerical *ERG* break-apart patterns (as described in *Materials and Methods*) are displayed in the bottom row. Fusion events are yellow, and patterns indicating normal *ERG* alleles are light blue. The four most frequently observed *ERG* break-apart patterns are displayed at the bottom right.

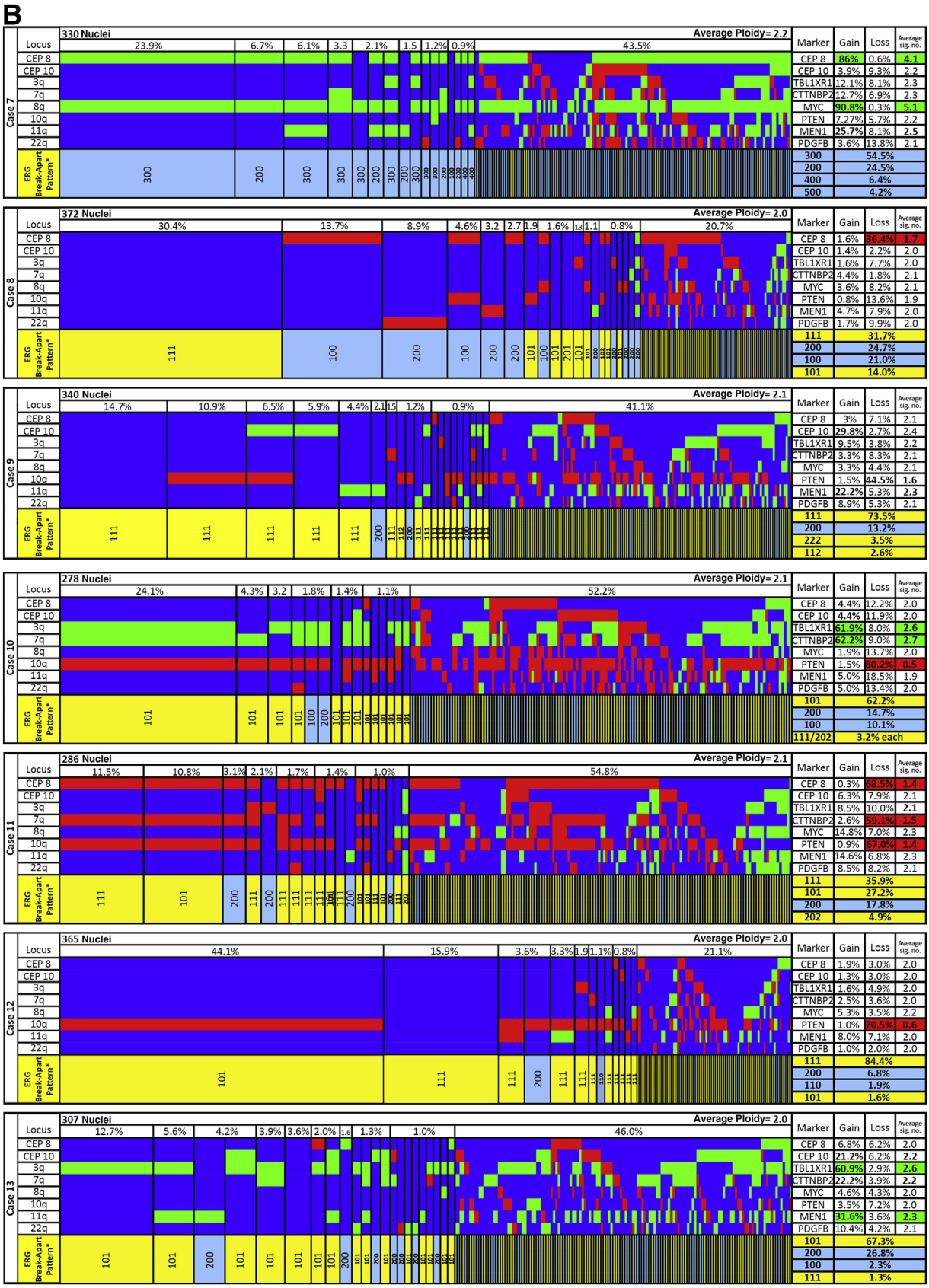

Figure 1 (*continued*).

Table 2 Summary of Results for Primary Prostate Carcinomas with and without Progressive Disease

Patient group	Case no.	Total no. of cells counted	Total no. of signal patterns	Instability index (no. of patterns × 100/no. of cells)	% Diploid cells (according to FISH signals)	DNA cytometry measurement		% Cells with *TMPRSS2* - *ERG* fusion	Major clonal imbalance patterns	Major clonal signal patterns
						Ploidy	Stem line			
Non-progressers	1	278	139	50	100.0	Euploid	1.92	80.2	19% Fusion, 9% Fusion + MEN1 gain	19% 22222222111
	2	382	226	59.2	70.9	Euploid	1.69	84.3	13% Fusion + MEN1 gain, 11% Fusion	7% 22222232011 4% 22222232101 2% 22222242011
	3	197	85	43.1	100.0	Euploid	1.96	23.4	12% Fusion, 11% No fusion + *MEN1* loss, 8% No fusion + *MEN1* gain	12% 22222222101
	4	336	208	61.9	67.0	Euploid	2	63.7	11% Fusion, 5% No fusion + *MEN1* gain, 4% Fusion + *MEN1* gain	7% 22222222101 3% 44444444202
	5	381	159	41.7	92.1	Euploid	2.01	80.8	28% Fusion + CEP8 loss, 4% Fusion + CEP8 loss + *MEN1* gain	28% 12222222111
	6	257	139	54.1	77.8	Euploid	2.02	60.7	16% Fusion + CEP8 loss, 5% No fusion + *CTTNBP2* loss, 4% Fusion + CEP8 loss + *CTTNBP2* gain	11% 12222222101 5% 24444444202
	Average	305.2	159.3	51.7	84.6	NA	1.93	65.5	Average size of major imbalance clone = 16.5%	Average size of major signal pattern clone = 14.0%
Progressers	7	330	212	64.2	88.7	Euploid	2	5.2	24% *ERG* gain + CEP8 gain + *MYC* (alias c-*myc*) gain, 6% *ERG* gain + CEP8 gain + *MYC* gain + *MEN1* gain	9% 42225222300 4% 32225222300 3% 42224222300
	8	372	96	25.8	97.6	Euploid	2.01	53.5	30% Fusion, 14% No fusion + CEP8 loss, 9% No fusion + *PDGFB* loss	30% 22222222111
	9	340	158	46.5	95.3	Euploid	2.01	84.1	15% Fusion, 11% Fusion + *PTEN* loss, 7% Fusion + CEP10 gain + *PTEN* loss	15% 22222222111
	10	278	157	56.5	96.4	ND	ND	73.7	24% Fusion + *TBL1XR1* gain + *CTTNBP2* gain + *PTEN loss*, 4% Fusion + *CTTNBP2* gain + *PTEN loss*	23% 22332022101
	11	287	161	56.1	94.8	Euploid	1.96	78.3	22% Fusion + CEP8 loss + *CTTNBP2* loss + *PTEN* loss, 3% No fusion + CEP8 loss + *CTTNBP2* loss + *PTEN* loss	11% 12212122111 11% 12212122101
	12	365	87	23.8	99.5	Euploid	1.96	90.7	44% Fusion + *PTEN* loss, 16% Fusion	44% 22222022111
	13	306	164	53.6	99.7	Euploid	1.96	71.0	13% Fusion + *TBL1XR1* gain, 6% Fusion + *TBL1XR1* gain + *MEN1* gain	12% 22322222101
	Average	325.4	147.9	46.6	96.0	NA	1.98	65.2	Average size of major imbalance clone = 24.6%	Average size of major signal pattern clone = 20.6%
Average for all cases		316.1	153.2	49	90.8	NA	NA	65.4	Average size of major clone = 20.8%	Average size of major signal pattern clone = 17.5%

NA, not applicable; ND, not determined.

signal number for each gene locus. The results for all 13 cases are displayed in Figure 1.

The most frequent imbalance clone in each tumor comprised, on average, 20.8% of the cell population, with a range of 11% to 44% (Figure 1 and Table 2). Interestingly, the average size of the major imbalance clone in the progressers was 24.6% (average size for major signal pattern clone, 20.6%), whereas the average size in non-progressers

Table 3 Overview of Gains and Losses Observed in >30% of Tumor Cells of the Six Non-Progressers and Seven Progressers

Patient group	Case no.	CEP8	CEP10	*TBL1XR1*	*CTTNBP2*	*MYC* (alias c-*myc*)	*PTEN*	*MEN1*	*PDGFB*
Non-progressers	1	—	—	—	—	—	—	—	—
	2	—	—	—	—	—	—	Gain	—
	3	—	—	—	—	—	—	—	—
	4	—	—	—	—	—	—	—	—
	5	Loss	—	—	—	—	—	—	—
	6	Loss	—	—	—	—	—	—	—
Progressers	7*	Gain	—	—	—	Gain	—	—	—
	8	Loss	—	—	—	—	—	—	—
	9*	—	—	—	—	—	Loss	—	—
	10*	—	—	Gain	Gain	—	Loss	—	—
	11*	Loss	—	—	Loss	—	Loss	—	—
	12*	—	—	—	—	—	Loss	—	—
	13*	—	—	Gain	—	—	—	Gain	—

—, neither a gain nor a loss occurs.
*Cases were detected by a three-probe panel consisting of FISH probes for *PTEN*, *MYC*, and *TBL1XR1*.

was only 16.5% (14% for major signal pattern clone), suggesting that progressers have a higher degree of selection for a specific clone. However, there were only slight differences in the average instability index measured as the number of FISH signal patterns per 100 cells (46.6 versus 51.7) and the average percentage cells with fusion for *TMPRSS2-ERG* (65.2% versus 65.5%) between samples from patients with or without progression (Table 2). Wilcoxon tests of the instability index, Shannon index, and Simpson index comparing non-progressers with progressers showed no statistically significant differences in these measures of heterogeneity. Also, nuclear ploidy measurements could not discern between non-progressers and progressers.

The major clones of all lesions showed fusion events of *TMPRSS2-ERG*, except for one progresser, which was the only case that displayed gains of *MYC* and CEP8, indicating a gain of the entire chromosome 8 (case 7) (Figure 1). This was also the only case with gains of a normal *ERG* allele; therefore, it might follow a different pathway to progressive disease. Four progressers, cases 9, 10, 11, and 12 (Figure 1), revealed major clones with *PTEN* loss, which was not observed in any of the non-progressers. In addition, case 9 had a major clone with only a fusion event for *TMPRSS2-ERG*. The remaining two progressers had major clones with either only a fusion event (case 8) (Figure 1) or a fusion event with a *TBL1RX1* gain (case 13) (Figure 1), respectively. The aberrations in the major clones of non-progressing tumors were fusion events only (cases 1, 3, and 4) (Figure 1), a fusion event with a *MEN1* gain (case 2) (Figure 1), and *TMPRSS2-ERG* fusion events with a CEP8 loss (cases 5 and 6) (Figure 1). Table 3 shows that overall more chromosomal gains and losses were found in carcinomas from the progresser group, whereas carcinomas of the non-progressing patients showed few changes, involving the loss of CEP8 and the gain of *MEN1*. Specifically, three gains/losses in the non-progresser group and 13 gains/losses in the progresser group are listed (Table 3). To evaluate whether the imbalance in the distribution is statistically significant, we permuted the entries in (a copy of) each column 10,000 times (Table 3). One can obtain an empirical one-sided P value by asking what proportion of the 10,000 scrambled replicates has, at most, three gains/losses in the non-progresser group and correspondingly at least 13 gains/losses in the progresser group. By using this permutation test, we obtained $P = 0.0143$.

TMPRSS2-ERG Fusion

In 12 of 13 lesions, the break-apart probe indicates clonal patterns with a *TMPRSS2-ERG* fusion. There was no significant difference in the average percentage of cells with fusion (65.2% versus 65.5%) between samples from patients with or without progression (Table 2). Most cases exhibited tumor cell populations that were heterogeneous for the *ERG* break-apart probe, often including a population with two normal alleles for *ERG* (pattern 200) (Figure 1). However, 6 of the 13 cases showed a specific fusion pattern in >60% of their tumor cell population, indicating that in those tumors either this was an early event in tumorigenesis or there was a strong selection for this particular pattern. There was no significant difference in the distribution of fusions by either insertion or translocation (pattern 111) and deletion (pattern 101) in the progressers and the non-progressers. Two non-progressers, but none of the progressers, revealed clonal cell populations with a double deletion of the sequences between *ERG* and *TMPRSS2* (cases 4 and 6) (Figure 1). However, the double deletion pattern 202 was observed in tetraploid cells, indicating a duplication of a diploid cell with the single deletion pattern 101. There was one progresser with a gain of a normal *ERG* allele (case 7). This case was also the only case with a gain of *MYC*.

Various studies have suggested that *ERG-TMPRSS2* fusions are early events in prostate cancer development.[20,64,65] In our samples, there were five cases (cases 1, 5, 9, 10, and 13) (Figure 1) that revealed clones with the same *ERG* break-apart pattern but different gain and loss patterns for the other genes analyzed, indicating that the *TMPRSS2-ERG* fusion

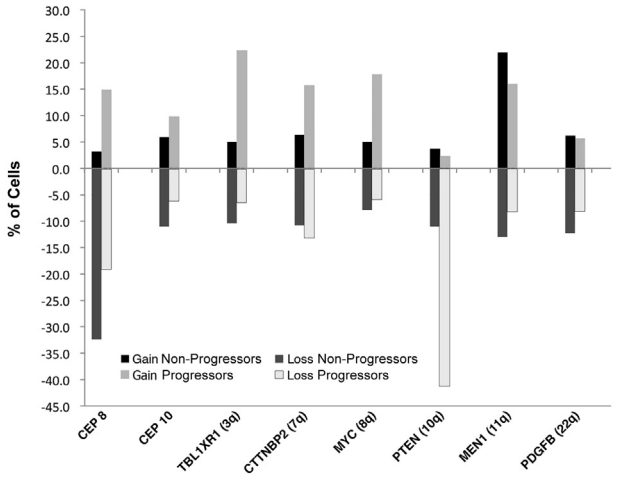

Figure 2 Average gain and loss frequencies for all of the gene markers and two centromere probes observed in prostate carcinoma cells of patients with and without progression. Percentages of cells with gains are shown above the 0% line and with losses below the 0% line.

happened as the first event, followed by specific chromosomal gains and losses. However, four cases (cases 2, 7, 8, and 11) (Figure 1) showed clones with the same gain and loss patterns, but different *ERG* break-apart patterns, which might indicate that the cells first acquired a specific chromosomal imbalance, and that the *TMPRSS2-ERG* fusion happened as a later event. In the remaining four cases (cases 3, 4, 6, and 12) (Figure 1), there were different *ERG* break-apart patterns with different gain and loss patterns, most likely indicating a parallel development of different clones. This is surprising because it appeared more likely that within one tumor focus, fusion status should be clonal, although interfocal heterogeneity in the *TMPRSS2-ERG* fusions of multifocal prostate tumors had been reported.[25] The 202 pattern in case 6 can be explained with a tetraploidization of the genome that resulted in a duplication of the 101 pattern seen in the major clone of this case.

Correlation of aCGH and FISH

The correlation between gains and losses called by aCGH and FISH was 83.3%[61] when using a threshold of >30% of the cells with gain or loss for FISH. Most of the discrepant calls are due to *CTTNBP2* gains called by aCGH but not seen by FISH, and *MEN1* gains seen by FISH but not called by aCGH.

DNA Ploidy Measurement Results

Image cytometry measuring the nuclear DNA content and determining the ploidy status did not reveal any aneuploid lesions among the six non-progresser and six of the seven progresser cases (one case did not have adequate material to be measured) (Table 2). All cases had diploid stem lines. A few cases showed small fractions of proliferating and/or tetraploid cells, which was in concordance with our FISH signal pattern observations (Table 2). In summary, all cases showed euploid DNA histograms indicating that DNA ploidy measurements were not able to discern non-progressers from progressers in our study.

Performance of the FISH Probes as Progression Markers

Figures 2 and 3 and Table 3 give a summary of the overall performance of the six gene markers and the two centromere probes tested with regard to differential gain and loss patterns in progressive and non-progressive prostate carcinomas. Figure 2 shows the average gain and loss frequencies for all of the gene markers and two centromere probes observed in all prostate carcinoma cells analyzed, grouped by patients with or without progression. The most frequent change observed affects *PTEN* in the progressive disease group with a loss in >40% of the cells, compared with only 11% of the non-progresser group. The progresser group showed, on average, a 10% to 15% higher percentage of cells with *TBLX1R1*, *CTTNBP2*, or *MYC* gain compared with the non-progressers. However, *MEN1* and *PDGFB* showed similar percentages for progressers and non-progressers. In fact, *MEN1* gain was more frequently observed in the cells of non-progressing carcinomas.

When using a threshold of >30% of the cells showing the aberration, lesions from patients with progressive disease had an average of 1.9 gains/losses for the probes tested, compared with a substantially lower average of 0.5 for tumors from patients without progression (Figure 3). By using the same threshold, the loss of *PTEN* was the most frequent aberration in the progressers (4/7 = 57%), and was not observed in non-progressers, confirming its potential as a marker for aggressive disease. *TBL1XR1* was gained in two of the seven progressers (29%), whereas none of the non-progressers showed changes in the copy number of this gene. One progresser had a gain of *CTTNBP2* and another progresser had a loss of this gene, whereas none of the non-progressers showed

		No. of Lesions with >30% of Cells with Specific Marker Gain or Loss	
Marker	Chromosomal Location	Non-Progressors (n = 6)	Progressors (n = 7)
CEP8 gain	**cen 8**	**0**	**1**
CEP8 loss	cen 8	2	2
CEP10 gain	**cen 10**	**0**	**0**
***TBL1XR1* gain**	**3q26.3**	**0**	**2**
***CTTNBP2* gain**	**7q31.2**	**0**	**1**
CTTNBP2 loss	7q31.2	0	1
***MYC* gain**	**8q24.2**	**0**	**1**
PTEN loss	10q23.2	0	4
***MEN1* gain**	**11q13.1**	**1**	**1**
***PDGFB* gain/loss**	**22q13.1**	**0**	**0**
Average gain/loss per lesion		0.5	1.9

Figure 3 Specific gains and losses observed in non-progressive and progressive prostate cancer disease. CEP8 and *CTTNBP2* were gained and lost. The thicknesses of the **arrows** reflect the percentage of change from non-progressive to progressive disease. The increase of lesions with a loss of *PTEN* is the most pronounced.

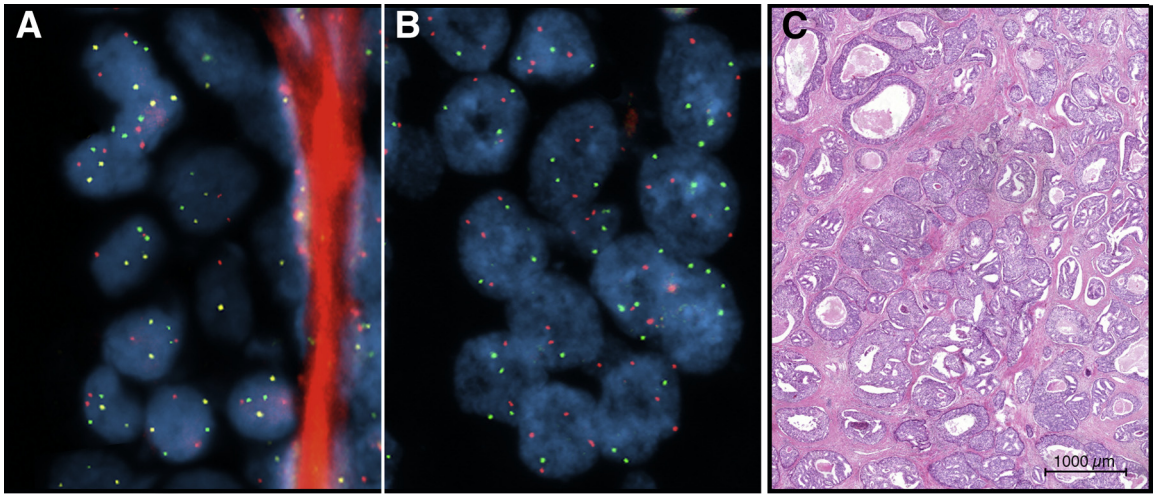

Figure 4 FISH on tissue sections with a prostate cancer–specific FISH probe panel. **A:** Normal prostate; most cells reveal two signals for the three probes [*MYC* (alias c-*myc*) in red, *TBLX1R1* in green, and *PTEN* in yellow]. Some cells are truncated because of sectioning. **B:** Prostate cancer; four copies for the probes *MYC* (red signals) and *TBL1XR1* (green signals) are present in most cells; again, cells are often truncated because of sectioning. We did not observe signals for the *PTEN*-specific probe, consistent with a biallelic deletion of this gene. **C:** Representative area of H&E-stained section of this cancer.

CTTNBP2 copy number changes. One progresser revealed CEP8 and *MYC* gains, indicative of a chromosome 8 gain. The gain of *MYC* was not observed in non-progressers. *MEN1* was gained in one progresser and one non-progresser lesion, whereas *PDGFB* was not changed in any of the lesions, indicating that these two genes are not differentially gained or lost in progressers. A probe set consisting of *PTEN*, *MYC*, and *TBL1XR1* would have detected six of the seven progressers analyzed, which is equivalent to a test sensitivity of 86% (Table 3). The one progresser case that would not have been detected (case 8) had a major clone (30% of the cell population) with a *TMPRSS2-ERG* fusion pattern of 111 and two minor clones, one comprising 12% of the cell population with an unusual *ERG* loss and a loss of CEP8 indicating an 8p loss and another clone comprising approximately 10% of the cell population revealing a rare loss of *PDGFB* on a normal diploid background without a *TMPRSS2-ERG* fusion (Figure 3). All non-progressers would have been negative for a test with a probe set of *PTEN, MYC*, and *TBL1XR1* (100% specificity), indicating that the combination of these three markers might have potential to predict progression in prostate carcinomas. By using the permutation test method described above, the combination of 86% sensitivity and 100% specificity has an empirical *P* value of 0.013.

Applying the *MYC-TBL1XR1-PTEN* Probe Panel to Tissue Sections of Prostate Cancers

We tested whether the three-color FISH probe panel that was determined to have the highest combined sensitivity and specificity (namely, *MYC-TBL1XR1-PTEN*) can be easily applied to routine tissue sections of FFPE material. We successfully hybridized three different prostate cancer specimens. The hybridizaton of one of the prostate cancer cases and the H&E stain for the tumor is shown in Figure 4. The tumor cells did not show any *PTEN* signal, indicative of a biallelic loss of *PTEN* (Figure 4B), whereas normal ducts in the neighboring tissue revealed a normal signal pattern with mostly two signals per nucleus and probe. Signal counts of fewer than two are most likely due to the truncation of cells (Figure 4A). *TBL1XR1* and *MYC* revealed mostly four signals per tumor nucleus, indicating a possible gain for both markers in the tumor cells (Figure 4B). We also observed truncation artifacts due to sectioning.

Tree Models of Tumor Progression Show a Different Pattern of Changes in Non-Progressers versus Progressers

Although, in this study, the instability indexes of the prostate carcinomas with or without progression after RP are similar, the frequency of genomic imbalances is substantially higher in the progresser group, with 1.9 gains or losses per case versus 0.5 gains or losses in the non-progressers. To visualize the pattern of progression in each case, we constructed tree models of progression using FISHtrees software, which infers phylogenetic trees describing likely evolution of the set

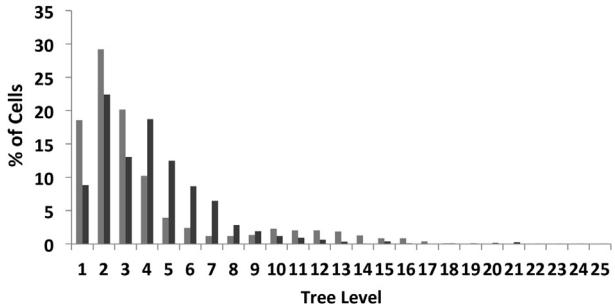

Figure 5 Distribution of cells across different levels of tumor progression trees for non-progresser (light gray bars) and progresser (dark gray bars) cases.

of observed signal counts within each tumor from an initially diploid root cell to heuristically minimize total copy number changes across the tree (Supplemental Figures S1–S13).[58] To evaluate whether there were statistically significant differences between the inferred phylogenetic trees of non-progressers versus progressers, the cell distribution across tree levels was calculated (Figure 5). The analysis showed that in the non-progressers, 70% of all cells were distributed within the first three tree levels, which was true for only 44% of the cells of the lesions that progressed. This observation indicates that cells of lesions that have a higher propensity to progress to advanced disease, on average, deviate more from the normal diploid status compared with cells from non-progressing lesions. This observation can be formalized statistically by computing weighted average depth of the nodes up to some level L for the six non-progressers and the seven progressers. The weighted average depths for $L = 5,\ldots 12$ for the two sets (non-progressers versus progressers) were compared by a Wilcoxon signed-rank test, which shows that the weighted average depth in the progressers is statistically significantly greater (Supplemental Table S1). For example, for $L = 10$, the P value of the test is 0.018. The node depth is the distance away from the normal signal count pattern (2,….,2) expressed in terms of the count of copy number changes. Thus, the cells in the progresser samples have in general a trend toward more total chromosomal changes. This trend is not captured by previously proposed measures of diversity (Shannon or Simpson index).[62]

Discussion

Men with slowly progressing prostate cancers could be treated with active surveillance approaches instead of immediate, more aggressive treatment, including surgery, which can have considerable adverse effects.[66] This subset of patients will become larger as populations age and more tumors are detected early by screening efforts. Distinguishing patients with aggressive or indolent prostate carcinomas would help in designing risk-adapted neoadjuvant and adjuvant treatments.

Herein, we used single-cell genetic analysis of copy number changes and chromosomal translocations on the basis of interphase cytogenetics (FISH) to understand genome dynamics in prostate tumors from patients with or without progression after RP. This allowed us to evaluate a set of genetic markers for their usefulness to predict progression, identify pathways of carcinogenesis, and examine patterns of genomic imbalances and clonal evolution. We used three FISH probe panels targeting six genes identified by aCGH to be differentially gained and lost in tumors that progressed compared with tumors that did not progress. In addition, the *TMPRSS2-ERG* fusion status was assessed in the same cells with a FISH *ERG* break-apart probe, and two centromere probes were hybridized as control probes. The sequential hybridization of these panels to intact nuclei prepared from prostate carcinomas enabled us to enumerate all probe counts in multiple individual cells.

The non-progressing prostate carcinomas revealed a slightly higher average chromosomal instability index, calculated as the number of distinct signal patterns per 100 cells, with an average of 51.7 patterns (range, 41.7 to 59.2), compared with the progressing lesions, with an average of 46.6 patterns (range, 23.8 to 64.2). The range in the non-progressing lesions was narrower because two progresser lesions showed substantially lower indices (23.8 and 25.8) than the rest of the group (46.5 to 64.2), reflecting the fact that these two lesions had large populations of a major stable clone comprising 44% and 30% of the total tumor population. We have previously observed a higher average chromosomal instability index in a multicolor FISH study comparing breast ductal carcinoma *in situ* (DCIS) to synchronous invasive ductal carcinomas (IDCs). We observed 62.3 patterns (range, 14.5 to 93.3) in the DCIS and 70.6 patterns (range, 49.7 to 98.0) in the IDC.[31] In the breast lesions, we never observed any signal pattern clone comprising >22% of the tumor cell population, with 7 of 26 cases showing no stable signal pattern clone (ie, <4% of the cells have the same signal pattern), whereas in the prostate carcinomas, 4 of 13 cases showed signal pattern clones comprising >22% of the cells, with a range from 7% to 44% cells (average size, 17.5%) for the major signal pattern clones in all cases.

Although the higher instability indices and smaller clone populations observed in the breast tumors could be due to the fact that a different set of genes was analyzed, there are indications of generally higher intratumor heterogeneity in breast tumors, especially because certain breast tumors showed major clones with aberrations in all eight breast cancer–specific genes assessed. None of the prostate cancers showed major clones with more than three aberrations in the six genes assessed for prostate cancer progression, which might be indicative of lower intratumor heterogeneity in prostate tumors. We are currently analyzing cervical cancers and high-grade cervical intraepithelial neoplasias with eight gene probes specific for cervical cancer and have observed much lower instability indices in these tumors compared with the breast tumors and prostate tumors (data not shown). Taken together, these observations might indicate that there are major differences in tumor heterogeneity and clonal development between different tumor entities.

Although the instability index values between the prostate carcinomas with or without progression are similar, the frequency of chromosomal gains and losses is substantially higher in the progresser group, with 1.9 gains or losses per case versus 0.5 gains or losses in the non-progressers. By using the same threshold of >30% of the tumor cell population exhibiting the aberration, breast tumors showed much higher gain and loss frequencies, with an average of 3.5 gains and losses per DCIS case and 4.6 gains and losses per IDC case.[31] The increase of aberrations in the more

advanced disease stages shows that, in both tumor entities, additional aberrations are acquired during progression of the disease.

Of the 13 prostate cancers investigated, 12 had major clonal cell populations with a *TMPRSS2-ERG* fusion and there was no significant difference in the average number of cells with a *TMPRSS2-ERG* fusion between prostate carcinoma cases with or without progression after RP. *TMPRSS2-ERG* fusion status could, therefore, not be used to discern progressers from non-progressers. This observation is in concordance with previous publications,[16,18] and our results need to be interpreted with caution for *ERG*-negative cases. One progresser lesion (case 7) did not have any fusion event, but instead overexpressed *ERG* by acquiring extra copies of a normal *ERG* allele. This case was also the only case with CEP8 and *MYC* gains, indicating that this cancer followed a different pathway. Interestingly, Toubaji et al[67] observed that increased gene copy number of *ERG*, but not *TMPRSS2-ERG* fusion, predicts outcome in prostate cancers. They found that the presence of extra copies of the *ERG* gene is significantly associated with recurrence, which is consistent with the observation that our only case with *ERG* gain (case 7) was actually a lesion from a patient who progressed.

Two non-progressers, but none of the progressers, revealed clonal cell populations with a double deletion of the sequences between *ERG* and *TMPRSS2* (cases 4 and 6) (Figure 1), an *ERG* pattern that was reported to correlate with worse outcome.[15] In our cases, the double-deletion pattern 202 happened in tetraploid cells, so the dosage effect in these cells is most likely similar to pattern 101 in diploid cells.

The most frequent aberration that we observed in prostate carcinomas that progressed was the loss of *PTEN* (Figure 3). Four of seven progressers had cell populations with >30% showing this loss, whereas none of the nonrecurrent cases reached this threshold. Loss of *PTEN* has been frequently shown to be associated with tumor progression, tumor aggressiveness, and disease recurrence[68,69] and appears to be a promising marker to distinguish between progressing and non-progressing prostate carcinomas.[32,70] Interestingly, Leinonen et al[38] observed that the loss of *PTEN* expression was associated with shorter progression-free survival in *ERG*-positive, but not in *ERG*-negative, cases. This is consistent with our findings, because all our cases with *PTEN* loss were *ERG* positive and progressers. Other gene markers that showed differential gain and loss patterns between progressers and non-progressers were *TBL1XR1* on 3q26, *CTTNBP2* on 7q31, and *MYC* on 8q24; however, this occurred to a much lesser degree than *PTEN* (Figure 3). Two of the markers, *MEN1* on 11q13 and *PDGFB* on 22q13, did not show any differential gain and loss between progressers and non-progressers in our FISH analysis. *MEN1* was gained in one non-progresser and one progresser, whereas none of the lesions showed *PDGFB* aberrations in >30% of the tumor cell population (Figure 3).

Herein, a probe set consisting of *PTEN*, *MYC*, and *TBL1XR1* detected six of the seven progressers (86% sensitivity). The only progresser case that would not have been detected had a major clone with a *TMPRSS2-ERG* fusion pattern of 111 only, so additional markers might be needed to identify similar cases. However, none of these three genomic markers would have been positive for non-progressers, which is equivalent to a test specificity of 100%. Therefore, the combination of these three markers shows potential to predict progression in prostate carcinomas with high specificity and sensitivity. We successfully hybridized this probe panel on tissue sections of prostate cancers and detected, in one of the cancer specimens tested, a biallelic deletion of *PTEN* (ie, no signal for *PTEN*) and possible gains of the other two markers. This demonstration of the probe panel on prostate cancer tissue sections indicates that the proposed test is feasible and can be useful in a routine pathological setting. We plan to evaluate this probe panel in a larger study to further explore the prospect for a single-cell FISH test for the identification of patients with prostate cancer predicted to have a poor prognosis after RP and, thus, candidates for adjuvant therapy.

Acknowledgments

We thank Yasuko Kobayashi and the Tissue Core (University of California, San Francisco) for assisting with sample acquisition, Dr. Jeff Simko for performing pathological analysis, Vy Ngo for performing aCGH data verification, Bernard Chen for providing expert help with the preparation of figures, Katja Klempt-Giessing for giving excellent support with nuclear DNA image cytometry measurements, Mona Legator and Ying Zhang for preparing FISH probes, Patty Kuo for taking FISH images, and Dr. Timo Gaiser for assessing the histological sections.

Supplemental Data

Supplemental material for this article can be found at *http://dx.doi.org/10.1016/j.ajpath.2014.06.030*.

References

1. Siegel R, Naishadham D, Jemal A: Cancer statistics, 2013. CA Cancer J Clin 2013, 63:11–30
2. Brawley OW: Prostate cancer epidemiology in the United States. World J Urol 2012, 30:195–200
3. Logothetis CJ, Gallick GE, Maity SN, Kim J, Aparicio A, Efstathiou E, Lin SH: Molecular classification of prostate cancer progression: foundation for marker-driven treatment of prostate cancer. Cancer Discov 2013, 3:849–861
4. Mousses S, Bubendorf L, Wagner U, Hostetter G, Kononen J, Cornelison R, Goldberger N, Elkahloun AG, Willi N, Koivisto P, Ferhle W, Raffeld M, Sauter G, Kallioniemi OP: Clinical validation of candidate genes associated with prostate cancer progression in the

CWR22 model system using tissue microarrays. Cancer Res 2002, 62:1256–1260
5. Malhotra S, Lapointe J, Salari K, Higgins JP, Ferrari M, Montgomery K, van de Rijn M, Brooks JD, Pollack JR: A tri-marker proliferation index predicts biochemical recurrence after surgery for prostate cancer. PLoS One 2011, 6:e20293
6. Vainio P, Mpindi JP, Kohonen P, Fey V, Mirtti T, Alanen KA, Perala M, Kallioniemi O, Iljin K: High-throughput transcriptomic and RNAi analysis identifies AIM1, ERGIC1, TMED3 and TPX2 as potential drug targets in prostate cancer. PLoS One 2012, 7: e39801
7. Roychowdhury S, Chinnaiyan AM: Advancing precision medicine for prostate cancer through genomics. J Clin Oncol 2013, 31: 1866–1873
8. Zellweger T, Sturm S, Rey S, Zlobec I, Gsponer JR, Rentsch CA, Terracciano LM, Bachmann A, Bubendorf L, Ruiz C: Estrogen receptor beta expression and androgen receptor phosphorylation correlate with a poor clinical outcome in hormone-naive prostate cancer and are elevated in castration-resistant disease. Endocr Relat Cancer 2013, 20:403–413
9. Tomlins SA, Rhodes DR, Perner S, Dhanasekaran SM, Mehra R, Sun XW, Varambally S, Cao X, Tchinda J, Kuefer R, Lee C, Montie JE, Shah RB, Pienta KJ, Rubin MA, Chinnaiyan AM: Recurrent fusion of TMPRSS2 and ETS transcription factor genes in prostate cancer. Science 2005, 310:644–648
10. Perner S, Demichelis F, Beroukhim R, Schmidt FH, Mosquera JM, Setlur S, Tchinda J, Tomlins SA, Hofer MD, Pienta KG, Kuefer R, Vessella R, Sun XW, Meyerson M, Lee C, Sellers WR, Chinnaiyan AM, Rubin MA: TMPRSS2:ERG fusion-associated deletions provide insight into the heterogeneity of prostate cancer. Cancer Res 2006, 66:8337–8341
11. Soller MJ, Isaksson M, Elfving P, Soller W, Lundgren R, Panagopoulos I: Confirmation of the high frequency of the TMPRSS2/ERG fusion gene in prostate cancer. Genes Chromosomes Cancer 2006, 45:717–719
12. Wang J, Cai Y, Ren C, Ittmann M: Expression of variant TMPRSS2/ERG fusion messenger RNAs is associated with aggressive prostate cancer. Cancer Res 2006, 66:8347–8351
13. Tu JJ, Rohan S, Kao J, Kitabayashi N, Mathew S, Chen YT: Gene fusions between TMPRSS2 and ETS family genes in prostate cancer: frequency and transcript variant analysis by RT-PCR and FISH on paraffin-embedded tissues. Mod Pathol 2007, 20:921–928
14. Mehra R, Tomlins SA, Shen R, Nadeem O, Wang L, Wei JT, Pienta KJ, Ghosh D, Rubin MA, Chinnaiyan AM, Shah RB: Comprehensive assessment of TMPRSS2 and ETS family gene aberrations in clinically localized prostate cancer. Mod Pathol 2007, 20: 538–544
15. Attard G, Clark J, Ambroisine L, Fisher G, Kovacs G, Flohr P, Berney D, Foster CS, Fletcher A, Gerald WL, Moller H, Reuter V, De Bono JS, Scardino P, Cuzick J, Cooper CS, Group TP: Duplication of the fusion of TMPRSS2 to ERG sequences identifies fatal human prostate cancer. Oncogene 2008, 27:253–263
16. Gopalan A, Leversha MA, Satagopan JM, Zhou Q, Al-Ahmadie HA, Fine SW, Eastham JA, Scardino PT, Scher HI, Tickoo SK, Reuter VE, Gerald WL: TMPRSS2-ERG gene fusion is not associated with outcome in patients treated by prostatectomy. Cancer Res 2009, 69:1400–1406
17. Park K, Tomlins SA, Mudaliar KM, Chiu YL, Esgueva R, Mehra R, Suleman K, Varambally S, Brenner JC, MacDonald T, Srivastava A, Tewari AK, Sathyanarayana U, Nagy D, Pestano G, Kunju LP, Demichelis F, Chinnaiyan AM, Rubin MA: Antibody-based detection of ERG rearrangement-positive prostate cancer. Neoplasia 2010, 12: 590–598
18. FitzGerald LM, Agalliu I, Johnson K, Miller MA, Kwon EM, Hurtado-Coll A, Fazli L, Rajput AB, Gleave ME, Cox ME, Ostrander EA, Stanford JL, Huntsman DG: Association of TMPRSS2-ERG gene fusion with clinical characteristics and outcomes: results from a population-based study of prostate cancer. BMC Cancer 2008, 8:230
19. Barwick BG, Abramovitz M, Kodani M, Moreno CS, Nam R, Tang W, Bouzyk M, Seth A, Leyland-Jones B: Prostate cancer genes associated with TMPRSS2-ERG gene fusion and prognostic of biochemical recurrence in multiple cohorts. Br J Cancer 2010, 102: 570–576
20. Clark J, Merson S, Jhavar S, Flohr P, Edwards S, Foster CS, Eeles R, Martin FL, Phillips DH, Crundwell M, Christmas T, Thompson A, Fisher C, Kovacs G, Cooper CS: Diversity of TMPRSS2-ERG fusion transcripts in the human prostate. Oncogene 2007, 26:2667–2673
21. Liu W, Ewing CM, Chang BL, Li T, Sun J, Turner AR, Dimitrov L, Zhu Y, Sun J, Kim JW, Zheng SL, Isaacs WB, Xu J: Multiple genomic alterations on 21q22 predict various TMPRSS2/ERG fusion transcripts in human prostate cancers. Genes Chromosomes Cancer 2007, 46:972–980
22. Zammarchi F, Boutsalis G, Cartegni L: 5′ UTR control of native ERG and of Tmprss2:ERG variants activity in prostate cancer. PLoS One 2013, 8:e49721
23. Furusato B, Tan SH, Young D, Dobi A, Sun C, Mohamed AA, Thangapazham R, Chen Y, McMaster G, Sreenath T, Petrovics G, McLeod DG, Srivastava S, Sesterhenn IA: ERG oncoprotein expression in prostate cancer: clonal progression of ERG-positive tumor cells and potential for ERG-based stratification. Prostate Cancer Prostatic Dis 2010, 13:228–237
24. Mertz KD, Horcic M, Hailemariam S, D'Antonio A, Dirnhofer S, Hartmann A, Agaimy A, Eppenberger-Castori S, Obermann E, Cathomas G, Bubendorf L: Heterogeneity of ERG expression in core needle biopsies of patients with early prostate cancer. Hum Pathol 2013, 44:2727–2735
25. Yoshimoto M, Ding K, Sweet JM, Ludkovski O, Trottier G, Song KS, Joshua AM, Fleshner NE, Squire JA, Evans AJ: PTEN losses exhibit heterogeneity in multifocal prostatic adenocarcinoma and are associated with higher Gleason grade. Mod Pathol 2013, 26: 435–447
26. Tao Y, Ruan J, Yeh SH, Lu X, Wang Y, Zhai W, et al: Rapid growth of a hepatocellular carcinoma and the driving mutations revealed by cell-population genetic analysis of whole-genome data. Proc Natl Acad Sci U S A 2011, 108:12042–12047
27. Navin N, Kendall J, Troge J, Andrews P, Rodgers L, McIndoo J, Cook K, Stepansky A, Levy D, Esposito D, Muthuswamy L, Krasnitz A, McCombie WR, Hicks J, Wigler M: Tumour evolution inferred by single-cell sequencing. Nature 2011, 472:90–94
28. Hou Y, Song L, Zhu P, Zhang B, Tao Y, Xu X, et al: Single-cell exome sequencing and monoclonal evolution of a JAK2-negative myeloproliferative neoplasm. Cell 2012, 148:873–885
29. Snuderl M, Fazlollahi L, Le LP, Nitta M, Zhelyazkova BH, Davidson CJ, Akhavanfard S, Cahill DP, Aldape KD, Betensky RA, Louis DN, Iafrate AJ: Mosaic amplification of multiple receptor tyrosine kinase genes in glioblastoma. Cancer Cell 2011, 20:810–817
30. Szerlip NJ, Pedraza A, Chakravarty D, Azim M, McGuire J, Fang Y, Ozawa T, Holland EC, Huse JT, Jhanwar S, Leversha MA, Mikkelsen T, Brennan CW: Intratumoral heterogeneity of receptor tyrosine kinases EGFR and PDGFRA amplification in glioblastoma defines subpopulations with distinct growth factor response. Proc Natl Acad Sci U S A 2012, 109:3041–3046
31. Heselmeyer-Haddad K, Berroa Garcia LY, Bradley A, Ortiz-Melendez C, Lee WJ, Christensen R, Prindiville SA, Calzone KA, Soballe PW, Hu Y, Chowdhury SA, Schwartz R, Schäffer AA, Ried T: Single-cell genetic analysis of ductal carcinoma in situ and invasive breast cancer reveals enormous tumor heterogeneity yet conserved genomic imbalances and gain of MYC during progression. Am J Pathol 2012, 181:1807–1822
32. Paris PL, Andaya A, Fridlyand J, Jain AN, Weinberg V, Kowbel D, Brebner JH, Simko J, Watson JEV, Volik S, Albertson DG, Pinkel D, Alers JC, van der Kwast TH, Vissers KJ, Schroder FH, Wildhagen MF, Febbo PG, Chinnaiyan AM, Pienta KJ, Carroll PR,

Rubin MA, Collins C, van Dekken H: Whole genome scanning identifies genotypes associated with recurrence and metastasis in prostate tumors. Hum Mol Genet 2004, 13:1303–1313
33. Jenkins RB, Qian J, Lieber MM, Bostwick DG: Detection of c-myc oncogene amplification and chromosomal anomalies in metastatic prostatic carcinoma by fluorescence in situ hybridization. Cancer Res 1997, 57:524–531
34. Sato H, Minei S, Hachiya T, Yoshida T, Takimoto Y: Fluorescence in situ hybridization analysis of c-myc amplification in stage TNM prostate cancer in Japanese patients. Int J Urol 2006, 13:761–766
35. Cairns P, Okami K, Halachmi S, Halachmi N, Esteller M, Herman JG, Jen J, Isaacs WB, Bova GS, Sidransky D: Frequent inactivation of PTEN/MMAC1 in primary prostate cancer. Cancer Res 1997, 57:4997–5000
36. Steck PA, Pershouse MA, Jasser SA, Yung WK, Lin H, Ligon AH, Langford LA, Baumgard ML, Hattier T, Davis T, Frye C, Hu R, Swedlund B, Teng DHR, Tavtigian SV: Identification of a candidate tumour suppressor gene, MMAC1, at chromosome 10q23.3 that is mutated in multiple advanced cancers. Nat Genet 1997, 15:356–362
37. Phin S, Moore MW, Cotter PD: Genomic rearrangements of PTEN in prostate cancer. Front Oncol 2013, 3:240
38. Leinonen KA, Saramaki OR, Furusato B, Kimura T, Takahashi H, Egawa S, Suzuki H, Keiger K, Ho Hahm S, Isaacs WB, Tolonen TT, Stenman UH, Tammela TL, Nykter M, Bova GS, Visakorpi T: Loss of PTEN is associated with aggressive behavior in ERG-positive prostate cancer. Cancer Epidemiol Biomarkers Prev 2013, 22: 2333–2344
39. Lapointe J, Li C, Giacomini CP, Salari K, Huang S, Wang P, Ferrari M, Hernandez-Boussard T, Brooks JD, Pollack JR: Genomic profiling reveals alternative genetic pathways of prostate tumorigenesis. Cancer Res 2007, 67:8504–8510
40. Zafarana G, Ishkanian AS, Malloff CA, Locke JA, Sykes J, Thoms J, Lam WL, Squire JA, Yoshimoto M, Ramnarine VR, Meng A, Ahmed O, Jurisca I, Milosevic M, Pintilie M, van der Kwast T, Bristow RG: Copy number alterations of c-MYC and PTEN are prognostic factors for relapse after prostate cancer radiotherapy. Cancer 2012, 118:4053–4062
41. Chandrasekharappa SC, Guru SC, Manickam P, Olufemi S-E, Collins FS, Emmert-Buck MR, Debelenko LV, Zhuang Z, Lubensky IA, Liotta LA, Crabtree JS, Wang Y, Roe BA, Weisemann J, Boguski MS, Agarwal SK, Kester MB, Kim YS, Heppner C, Dong Q, Spiegel AM, Burns AL, Marx SJ: Positional cloning of the gene for multiple endocrine neoplasia-type 1. Science 1997, 276:404–407
42. Seigne C, Fontanière S, Carreira C, Lu J, Tong W-M, Fontanière B, Wang Z-Q, Zhang CX, Frappart L: Characterisation of prostate cancer lesions in heterozygous Men1 mutant mice. BMC Cancer 2010, 10:395
43. Paris PL, Sridharan S, Hittelman AB, Kobayashi Y, Perner S, Huang G, Simko J, Carroll P, Rubin MA, Collins C: An oncogenic role for the multiple endocrine neoplasia type 1 gene in prostate cancer. Prostate Cancer Prostatic Dis 2009, 12:184–191
44. Lapointe J, Li C, Higgins JP, van de Rijn M, Bair E, Montgomery K, Ferrari M, Egevad L, Rayford W, Bergerheim U, Ekman P, DeMarzo AM, Tibshirani R, Botstein D, Brown PO, Brooks JD, Pollack JR: Gene expression profiling identifies clinically relevant subtypes of prostate cancer. Proc Natl Acad Sci U S A 2004, 101: 811–816
45. Zhang XM, Chang Q, Zeng L, Gu J, Brown S, Basch RS: TBLR1 regulates the expression of nuclear hormone receptor co-repressors. BMC Cell Biol 2006, 7:31
46. Li J, Wang CY: TBL1-TBLR1 and beta-catenin recruit each other to Wnt target-gene promoter for transcription activation and oncogenesis. Nat Cell Biol 2008, 10:160–169
47. Daniels DL, Weis WI: Beta-catenin directly displaces Groucho/TLE repressors from Tcf/Lef in Wnt-mediated transcription activation. Nat Struct Mol Biol 2005, 12:364–371
48. Robinson DR, Zylstra CR, Williams BO: Wnt signaling and prostate cancer. Curr Drug Targets 2008, 9:571–580
49. Liu Y, Sun W, Zhang K, Zheng H, Ma Y, Lin D, Zhang X, Feng L, Lei W, Zhang Z, Guo S, Han N, Tong W, Feng X, Gao Y, Cheng S: Identification of genes differentially expressed in human primary lung squamous cell carcinoma. Lung Cancer 2007, 56: 307–317
50. Gonzalez-Aguilar A, Idbaih A, Boisselier B, Habbita N, Rossetto M, Laurenge A, Bruno A, Jouvet A, Polivka M, Adam C, Figarella-Branger D, Miquel C, Vital A, Ghesquières H, Gressin R, Delwail V, Taillandier L, Chinot O, Soubeyran P, Gyan E, Choquet S, Houillier C, Soussain C, Tanguy ML, Marie Y, Mokhtari K, Hoang-Xuan K: Recurrent mutations of MYD88 and TBL1XR1 in primary central nervous system lymphomas. Clin Cancer Res 2012, 18: 5203–5211
51. Heldin CH, Westermark B: Mechanism of action and in vivo role of platelet-derived growth factor. Physiol Rev 1999, 79:1283–1316
52. Chott A, Sun Z, Morganstern D, Pan J, Li T, Susani M, Mosberger I, Upton MP, Bubley GJ, Balk SP: Tyrosine kinases expressed in vivo by human prostate cancer bone marrow metastases and loss of the type 1 insulin-like growth factor receptor. Am J Pathol 1999, 155: 1271–1279
53. Singh D, Febbo PG, Ross K, Jackson DG, Manola J, Ladd C, Tamayo P, Renshaw AA, D'Amico AV, Richie JP, Lander ES, Loda M, Kantoff PW, Golub TR, Sellers WR: Gene expression correlates of clinical prostate cancer behavior. Cancer Cell 2002, 1: 203–209
54. Conley-LaComb MK, Huang W, Wang S, Shi D, Jung YS, Najy A, Fridman R, Bonfil RD, Cher ML, Chen YQ, Kim HR: PTEN regulates PDGF ligand switch for beta-PDGFR signaling in prostate cancer. Am J Pathol 2012, 180:1017–1027
55. Chen YK, Hsueh YP: Cortactin-binding protein 2 modulates the mobility of cortactin and regulates dendritic spine formation and maintenance. J Neurosci 2012, 32:1043–1055
56. Panigrahi AK, Zhang N, Otta SK, Pati D: A cohesin-RAD21 interactome. Biochem J 2012, 442:661–670
57. Coolen MW, Stirzaker C, Song JZ, Statham AL, Kassir Z, Moreno CS, Young AN, Varma V, Speed TP, Cowley M, Lacaze P, Kaplan W, Robinson MD, Clark SJ: Consolidation of the cancer genome into domains of repressive chromatin by long-range epigenetic silencing (LRES) reduces transcriptional plasticity. Nat Cell Biol 2010, 12:235–246
58. Chowdhury SA, Shackney SE, Heselmeyer-Haddad K, Ried T, Schäffer AA, Schwartz R: Phylogenetic analysis of multiprobe fluorescence in situ hybridization data from tumor cell populations. Bioinformatics 2013, 29:i189–i198
59. Wangsa D, Heselmeyer-Haddad K, Ried P, Eriksson E, Schäffer AA, Morrison LE, Luo J, Auer G, Munck-Wikland E, Ried T, Lundqvist EÅ: Fluorescence in situ hybridization markers for prediction of cervical lymph node metastases. Am J Pathol 2009, 175: 2637–2645
60. Auer GU, Caspersson TO, Wallgren AS: DNA content and survival in mammary carcinoma. Anal Quant Cytol 1980, 2:161–164
61. Paris PL, Weinberg V, Albo G, Roy R, Burke C, Simko J, Carroll P, Collins C: A group of genome-based biomarkers that add to a Kattan nomogram for predicting progression in men with high-risk prostate cancer. Clin Cancer Res 2010, 16:195–202
62. Park SY, Gonen M, Kim HJ, Michor F, Polyak K: Cellular and genetic diversity in the progression of in situ human breast carcinomas to an invasive phenotype. J Clin Invest 2010, 120: 636–644
63. D'Amico AV, Whittington R, Malkowicz SB, Schultz D, Blank K, Broderick GA, Tomaszewski JE, Renshaw AA, Kaplan I, Beard CJ, Wein A: Biochemical outcome after radical prostatectomy, external beam radiation therapy, or interstitial radiation therapy for clinically localized prostate cancer. JAMA 1998, 280:969–974

64. Perner S, Mosquera JM, Demichelis F, Hofer MD, Paris PL, Simko J, Collins C, Bismar TA, Chinnaiyan AM, De Marzo AM, Rubin MA: TMPRSS2-ERG fusion prostate cancer: an early molecular event associated with invasion. Am J Surg Pathol 2007, 31:882–888
65. Mosquera JM, Perner S, Genega EM, Sanda M, Hofer MD, Mertz KD, Paris PL, Simko J, Bismar TA, Ayala G, Shah RB, Loda M, Rubin MA: Characterization of TMPRSS2-ERG fusion high-grade prostatic intraepithelial neoplasia and potential clinical implications. Clin Cancer Res 2008, 14:3380–3385
66. Steineck G, Helgesen F, Adolfsson J, Dickman PW, Johansson JE, Norlén BJ, Holmberg L; Scandinavian Prostatic Cancer Group Study Number 4: Quality of life after radical prostatectomy or watchful waiting. N Engl J Med 2002, 347:790–796
67. Toubaji A, Albadine R, Meeker AK, Isaacs WB, Lotan T, Haffner MC, Chaux A, Epstein JI, Han M, Walsh PC, Partin AW, De Marzo AM, Platz EA, Netto GJ: Increased gene copy number of ERG on chromosome 21 but not TMPRSS2-ERG fusion predicts outcome in prostatic adenocarcinomas. Mod Pathol 2011, 24:1511–1520
68. Chaux A, Peskoe SB, Gonzalez-Roibon N, Schultz L, Albadine R, Hicks J, De Marzo AM, Platz EA, Netto GJ: Loss of PTEN expression is associated with increased risk of recurrence after prostatectomy for clinically localized prostate cancer. Mod Pathol 2012, 25:1543–1549
69. Krohn A, Diedler T, Burkhardt L, Mayer PS, De Silva C, Meyer-Kornblum M, Kötschau D, Tennstedt P, Huang J, Gerhauser C, Mader M, Kurtz S, Sirma H, Saad F, Steuber T, Graefen M, Plass C, Sauter G, Simon R, Minner S, Schlomm T: Genomic deletion of PTEN is associated with tumor progression and early PSA recurrence in ERG fusion-positive and fusion-negative prostate cancer. Am J Pathol 2012, 181:401–412
70. Punnoose E, Tucker E, Marrinucci D, Amler LC, Koeppen H, Patel PH, Yan Y, Riisnaes R, Attard G, Sebastian De Bono J: Evaluation of PTEN status in circulating tumor cells (CTCs) and matched tumor tissue from patients with castrate-resistant prostate cancer (CRPC): 2013 Genitourinary Cancers Symposium. J Clin Oncol 2013, Abstract 62